Modeling and study of the arterial blood flow loaded with nanoparticles under squeezing action in presence of a magnetic field

Manar ENNAOURI, El-Kaber HACHEM*

Innovative Research and Applied Physics Team (RIPA), Faculty of Sciences, Moulay Ismail University,Meknes, Morocco.

Abstract. This article is intended to study the arterial blood flow with nanoparticles in a magnetic field due to the squeezing action of the heart, the study was treated as acasson nanofluid flowing between two parallel plates placed at a distance varying in time and under the influence of a uniform magnetic field with variable chemical reaction.Considering the following effects: viscous dissipation, generation of heat due to friction caused by shear in the flow, joule heating, brownian motion, and the influence of thermo-diffusion.Homotopy Perturbation Method is used to solve the nonlinear differential equations governing the problem. To verify the accuracy of the analytical method used, the results of the homotopy perturbation method (HPM) are compared with the results of the Numerical method using the fourth-order Runge–Kutta method (RK-4) and other results obtained in previous works so that the high accuracy of results is clear. Flow behaviour under the modifying involved physical parameters is also discussed and explained in detail in the form of graphs and tables. Through this study it is observed that magnetic field can be used as a control phenomenon in many flows as it normalizes the flow behaviour. Also, it is shown that positive and negative squeeze numbers have opposite effects on heat and mass transfer flow throughout all the cases. Further, the concentration field is a decreasing function of thermophoresis parameter. While, concentration profile enhances with raising brownian motion parameter. And various other important parameters were analyzed. Findings from this study can help engineers to improve and researchers to investigate faster and easier.

Keywords: Blood flow, Nanoparticles, Casson nanofluid, squeezing flow, Homotopyperturbationmethod (HPM), Runge–Kutta fourth-order method (RK-4).

*Correspondingauthor:hachem.elkaber@gmail.com

1 Introduction

Nanofluid is an advanced fluid with improved thermophysical properties that has been introduced in many applications for a better heat transfer process like nuclear reactors, biomedical applications (cancer therapeutics, cryopreservation, and nanodrug delivery) [1] .The term "nanofluids" was introduced by Choi and Eastman [2] and refers to a base fluid have a low thermal conductivity such as water, ethylene glycol etc with suspended solid nanoparticles having high thermal conductive metals, such as, copper, aluminum, etc. modelling nanofluid flow and heat transfer can be classified into two main groups: single-phase and two-phase model. In the single-phase model,the combination of nanoparticle and base fluid is considered as a single-phase mixture and the motion slip between nanoparticles and base fluid is not considered while, in the two-phase model, the nanoparticles cannot accompany fluid molecules due to certain slip mechanisms such as Brownian motion and thermophoresis, so the volume fraction of nanofluid may not be uniform anymore, and there would be a variable concentration of nanoparticles in a mixture. Since then, a large number of studies have been carried out on nanofluids in various aspects [3-5].

Recently, the investigation of heat and mass transfer squeezing flow known a great attention because of its various applications. The first work in this sector was reported by Stefan [6] using lubrication approximation. After Stefan's work, many researchers studied these flows for different cases and geometries. Domairry and Aziz were study the analytical solution for the squeezing flow of viscous fluid between parallel disks took into account the effects of suction or injection at the walls [7]. The squeezing flow over a porous surface has been addressed by Mahmood et al [8]. the combined effect of heat and mass transfer in the squeeze flow between parallel plates considering the viscous dissipation and chemical reaction effects was investigated by Mustafa et al [9].Further, Dagonchi and Ganji studied the MHD nanofluid flow and heat transfer in a stretching/shrinking convergent/divergent channel considering thermal radiation [10].Furthermore, the heat transfer and nanofluid flow between two parallel plates in a rotating system were studied by Sheikholeslami et al [11].

In real industrial applications, non-Newtonian fluids are more convenient to use than Newtonian fluids like human blood, shampoos, condensed milk, paints, and tomato paste, etc. non-Newtonian fluids show different characters which cannot be understood by Newtonian theory. In a Newtonian fluid, the relationship between the shear stress and the shear rate is linear, passing through the origin, the constant of proportionality being the coefficient of viscosity. However, in a non-Newtonian fluid, the relationship between the shear stress and the shear rate is different. The fluid can even exhibit viscosity as a function of time. Consequently, a constant viscosity coefficient cannot be defined. To fill out this gap, many non-Newtonian models have been proposed on various physical aspects.

Casson fluid is the preferred fluid among all non-Newtonian fluids.Among so many applications of the Casson fluid model, blood flow in the arteries is a common example ,and its formulation can be obtained from [12], and several studies have been presented of Casson fluid.Eldabe and Elmohands [13] and Boyd et al. [14] have studied the Casson fluid for the flow between two rotating cylinders [13] and for the steady and oscillatory blood flow [14].Fredrickson studied the steady flow of a Casson fluid in a tube [15], Mustafa et al investigated unsteady Boundary Layer Flow of a Casson Fluid Due to an Impulsively Started Moving Flat Plate [16].

Motivated by the above investigations, the main objective of this present paper is to study the arterial blood flow with nanoparticles in a magnetic field due to the squeezing action of the heart, the study was treated as acasson nanofluid flowing between two parallel plates placed at a distance varying in time and under the influence of a uniform magnetic field with variable chemical reaction.Taking into consideration the viscous dissipation effect, the generation of heat due to friction caused by shear in the flow, Joule heating, Brownian motion, and thermophoresis effect with time-dependent chemical reaction. the most important engineering problems, particularly heat transfer equations are nonlinear problems, so some they are solved using numerical methods and some are solved using different analytical methods.This article examines both numerical and analytical approaches. Analytical methods adopted by researchers in this sector include: differential transformation method DTM [17, 18] variation of parameter method VPM [19], homotopy analysis method HAM [9, 20], adomian decomposition method ADM [21], homotopy perturbation method HPM [22]. The analytical simulation method that does not need small parameters is the HPM, this method proposed and improved by He [23]. In this method, the solution is taken as the sum of an infinite series which usually converges quickly to the exact solution. Consequently, in this article the reduced ordinary differential equations have been solved by homotopy perturbation method HPM.The results of the homotopy perturbation method (HPM) are compared with the results of the Numerical method using the fourth-order Runge–Kutta method (RK-4) and other results obtained in previous works so that the high accuracy of results is clear.

2 Mathematical model

In this Section, let us consider the heat and mass transfer analysis in the unsteady two-dimensional squeezing flow of an incompressible viscous Casson nanofluid treated as blood with nanoparticles between two infinite parallel plates treated as the artery because the movement of arterial blood flow is a movement through thin spaces that can be thought of as a flow between parallel plates.As shown in**Fig.1** the two plates separated by a distance $y = \pm h(t) = \pm l(1 - at)^{\frac{1}{2}}$,

where l is the initial location (when time t=0) for $\alpha > 0$ the two plates are squeezed until they touch $t = 1/\alpha$ and for $\alpha < 0$ the two plates are separated. The effect of gravity is neglected,a uniform magnetic field is assumed to be applied towards direction y. The magnetic Reynolds number is assumed small, so the induced magnetic field can be negligible in comparison to the applied magnetic field. Consequently, the electric current and the electromagnetic force are defined by:

$\vec{J} = \sigma(\vec{v} \times \vec{B})$, $\vec{F} = \vec{J} \times \vec{B}$ then $\vec{F} = \sigma(\vec{v} \times \vec{B}) \times \vec{B}$.

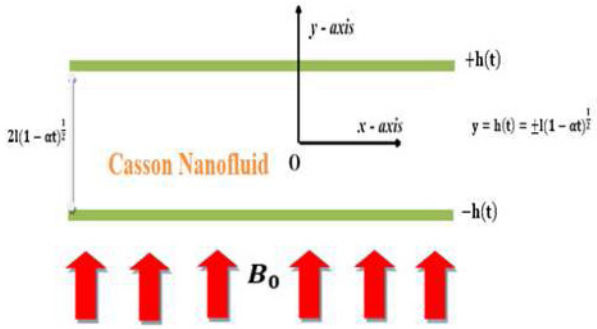

Fig. 1: Geometry of the problem

The rheological equation of state for an isotropic flow of a Casson fluid can be expressed as [12, 24]:

$$\tau_{ij} = \begin{cases} 2\left(\mu_B + \frac{p_y}{\sqrt{2\pi}}\right)e_{ij}, \pi > \pi_c \\ 2\left(\mu_B + \frac{p_y}{\sqrt{2\pi_c}}\right)e_{ij}, \pi < \pi_c \end{cases} \quad (1)$$

Where τ_{ij} is the $(i, j)^{th}$component of stress tensor, $\pi = e_{ij}e_{ij}$describes the product of deformation components, e_{ij} indicates the deformation rate on the $(i, j)^{th}$component, π_c shows the critical value. The dynamic plastic viscosity of Casson fluid is denoted by μ_B and p_y represents the yield stress.The deformation rate is equal to:

$$e_{ij} = \frac{1}{2}\left(\frac{\partial u_i}{\partial x_j} + \frac{\partial u_j}{\partial x_i}\right) \quad (2)$$

The equations governing the Casson nanofluid flow for conservation of mass, momentum, thermal energy, and nanoparticle concentration of this problem are written as [9, 10, 12, and 14]:

$$\frac{\partial u}{\partial x} + \frac{\partial v}{\partial y} = 0 \quad (3)$$

$$\frac{\partial u}{\partial t} + \left(u\frac{\partial u}{\partial x} + v\frac{\partial u}{\partial y}\right) = -\frac{1}{\rho_{nf}}\frac{\partial p}{\partial x} + \frac{\mu_{nf}}{\rho_{nf}}\left(1 + \frac{1}{\beta}\right)\left(2\frac{\partial^2 u}{\partial x^2} + \frac{\partial^2 u}{\partial y^2} + \frac{\partial^2 v}{\partial y \partial x}\right) - B_0^2\frac{\sigma_{nf}}{\rho_{nf}}u \quad (4)$$

$$\frac{\partial v}{\partial t} + \left(u\frac{\partial v}{\partial x} + v\frac{\partial v}{\partial y}\right) = -\frac{1}{\rho_{nf}}\frac{\partial p}{\partial y} + \frac{\mu_{nf}}{\rho_{nf}}\left(1 + \frac{1}{\beta}\right)\left(2\frac{\partial^2 v}{\partial y^2} + \frac{\partial^2 v}{\partial x^2} + \frac{\partial^2 u}{\partial y \partial x}\right) \quad (5)$$

$$\left(\frac{\partial T}{\partial t} + u\frac{\partial T}{\partial x} + v\frac{\partial T}{\partial y}\right) = \frac{k_{nf}}{(\rho c_p)_{nf}}\left(\frac{\partial^2 T}{\partial x^2} + \frac{\partial^2 T}{\partial y^2}\right) + B_0^2\frac{\sigma_{nf}}{(\rho c_p)_{nf}}u^2 + \frac{\mu_{nf}}{(\rho c_p)_{nf}}\left(1 + \frac{1}{\beta}\right)\left[4\left(\frac{\partial u}{\partial x}\right)^2 + \left(\frac{\partial u}{\partial y} + \frac{\partial v}{\partial x}\right)^2\right] + \frac{(\rho c_p)_p}{(\rho c_p)_{nf}}\left[D_B\left(\frac{\partial C}{\partial x}\frac{\partial T}{\partial x} + \frac{\partial C}{\partial y}\frac{\partial T}{\partial y}\right) + \frac{D_T}{T_\infty}\left(\frac{\partial T}{\partial x}\frac{\partial T}{\partial x} + \frac{\partial T}{\partial y}\frac{\partial T}{\partial y}\right)\right] \quad (6)$$

$$\frac{\partial C}{\partial t} + u\frac{\partial C}{\partial x} + v\frac{\partial C}{\partial y} = D_B\left(\frac{\partial^2 C}{\partial x^2} + \frac{\partial^2 C}{\partial y^2}\right) + \frac{D_T}{T_\infty}\left(\frac{\partial^2 T}{\partial x^2} + \frac{\partial^2 T}{\partial y^2}\right) - G(t)C \quad (7)$$

The boundary conditions are:

$$u = 0,\ v = v_w = \frac{dh}{dt},\ T = T_H, C = C_H \text{ at } y = h(t) \quad (8)$$

$$v = \frac{du}{dy} = \frac{dT}{dy} = \frac{dC}{dy} = 0 \text{ at } y = 0 \quad (9)$$

Where u and v are the velocities in the x and y directions respectively, T is the temperature, P is the pressure, σis the electric conductivity,K is the effect thermal conductivity,C is the concentration,μ is the dynamic viscosity, $D_B$andD_T are the Brownian motion coefficient and the thermophoretic diffusion coefficient, $T_\infty$is the mean fluid temperature ,$\beta = \frac{\mu_B\sqrt{2\pi_c}}{p_y}$ is the Casson fluid parameter and $G(t) = \frac{g}{(1-\alpha t)}$(see [25]) is the time-dependent reaction rate.

The following dimensionless groups are introduced:

$$\eta = \frac{y}{l(1-\alpha t)^{\frac{1}{2}}} = \frac{y}{h(t)}, u = \frac{x\alpha}{2(1-\alpha t)}f'(\eta), v = -\frac{\alpha l}{2(1-\alpha t)^{\frac{1}{2}}}f(\eta), \Theta = \frac{T}{T_H} \quad (10)$$

Substituting the above parameters into equations **3** to **7** the resulting equations give:

$$\left(1 + \frac{1}{\beta}\right)f''''(\eta) - S[\eta f'''(\eta) + f'(\eta)f''(\eta) - f(\eta)f'''(\eta) + 3f''(\eta)] - {H_a}^2 f''(\eta) = 0 \quad (11)$$

$$\Theta'' + (N_b)(\Theta'\varphi') + (N_t)\Theta'^2 + (P_r E_c)\left(1 + \frac{1}{\beta}\right)(f''^2 + 4\delta^2 f'^2) + (P_r S)(f\Theta' - \eta\Theta') + {H_a}^2 f'^2(\eta) = 0 \quad (12)$$

$$\varphi'' + (S_c S)(f\varphi' - \eta\varphi') + \left(\frac{N_t}{N_b}\right)\Theta'' - S_c G_r \varphi = 0 \quad (13)$$

The boundary condition in the new similar variables becomes:

$$f''(0) = 0, f(0) = 0, \theta'(0) = 0, \varphi'(0) = 0 \ \ at \ \ \eta = 0 \quad (14)$$

$$f'(1) = 0, f(1) = 1, \theta(1) = \varphi(1) = 1 \ at \ \eta = 1 \quad (15)$$

Where S is the squeeze number, H_a is the Hartmann number, N_b is the Brownian motion parameter,N_t is the thermophoretic parameter, P_r is the Prandtl number,$S_c$is the Schmidt number andG_r the chemical reaction parameter which are defined as:

$$S = \frac{\alpha l^2}{2\upsilon}, P_r = \frac{\mu c_p}{K}, \delta = \frac{l}{x}, Ha = \sqrt{\frac{l^2\sigma}{\mu}}B_0^2, Ec = \frac{1}{c_p}\left(\frac{\alpha x}{2(1-\alpha t)}\right)^2, Nb = \frac{(\rho c_p)_p D_B C_H}{(\rho c_p)_f K}, Nt = \frac{(\rho c_p)_p D_T T_H}{(\rho c_p)_f K}, Sc = \frac{\upsilon}{D_B}, G_r = \frac{gl^2}{\upsilon}$$

It is necessary to notice that the squeeze number S describes the movement of the plates ($S > 0$ corresponds to the plates moving separate, whereas $S < 0$ corresponds to the plates moving together this type of flow is called squeezing flow) [26,27]. Moreover, it should be mentioned that $E_c = 0 \text{and} H_a = 0$, corresponds to the case when the viscous dissipation and the magnetic force effect are absent. whereas, the Prandtl number is used to evaluate the velocity with which momentum and energy propagates through the nanofluid and the Schmidt number is used to characterize fluid flows in which there are simultaneous momentum and mass transfer processes in addition to $G_r > 0$ represents the destructive chemical reaction and $G_r < 0$ characterizes the generative chemical reaction [9,25].

3 Homotopy perturbation technique

We can construct Homotopy functions for the Equations **(11)-(13)** governing the problem as shown in reference[28], we get:

$$H(f,p) = (1-p)\left[\left(1+\frac{1}{\beta}\right)f'''' - \left(1+\frac{1}{\beta}\right){f_0}''''(0)\right] + p[f'''' + S(ff''' - 3f'' - \eta f''' - f'f'') - Ha^2 f''] = 0 \quad (16)$$

$$H(\theta,p) = (1-p)[\Theta'' - {\Theta_0}''(0)] + p\left[\theta'' + (N_b)(\Theta'\varphi') + (N_t)\Theta'^2 + (P_r E_c)\left(1+\frac{1}{\beta}\right)(f''^2 + 4\delta^2 f'^2) + (P_r S)(f\Theta' - \eta\Theta') + {H_a}^2 f'^2(\eta)\right] = 0 \quad (17)$$

$$H(\varphi,p) = (1-p)[\varphi'' - {\varphi_0}''(0)] + p\left[\varphi'' + (S_c S)(f\varphi' - \eta\varphi') + \left(\frac{N_t}{N_b}\right)\Theta'' - S_c G_r \varphi\right] \quad (18)$$

We consider f and θ as follows:

$$f(\eta) = f_0(\eta) + p^1 f_1(\eta) + p^2 f_2(\eta) + \cdots = \sum_{i=0}^{N} p^i f_i(\eta) \quad (19)$$

$$\theta(\eta) = \theta_0(\eta) + p^1\theta_1(\eta) + p^2\theta_2(\eta) + \cdots = \sum_{i=0}^{N} p^i f_i\theta_i(\eta) \quad (20)$$

$$\varphi(\eta) = \varphi_0(\eta) + p^1\varphi_1(\eta) + p^2\varphi_2(\eta) + \cdots = \sum_{i=0}^{N} p^i\varphi_i(\eta) \quad (21)$$

With substituting f, θ and φ from equations **(19-21)** into equations **(10-12)** and some simplification and rearranging based on powers of$p-terms$, we have:

$\boldsymbol{p^0}$: (22)

$${f_0}'''' = 0, {\theta_0}'' = 0, {\varphi_0}'' = 0$$

The boundary conditions are:

$$f''(0) = 0, f(0) = 0, \theta'(0) = 0, \phi'(0) = 0 \; at \; \eta = 0 \quad (23)$$

$$f'(1) = 0, f(1) = 1, \theta(1) = \phi(1) = 1 \; at \; \eta = 1 \quad (24)$$

$\boldsymbol{p^1}$: (25)

$${f_1}'''' + S({f_0}{f_0}''' - 3{f_0}'' - \eta{f_0}''' - {f_0}'{f_0}'') - Ha^2{f_0}'' = 0$$

$${\theta_1}'' + (P_r E_c)\left({f_0}''^2 + 4\delta^2{f_0}'^2\right) + (P_r S)({f_0}{\theta_0}' - \eta{\theta_0}') + (N_b)({\theta_0}'{\varphi_0}') + (N_t){\theta_0}'^2 + {H_a}^2{f_0}'^2(\eta) = 0$$

$${\varphi_1}'' + (S_c S)({f_0}{\varphi_0}' - \eta{\varphi_0}') + \left(\frac{N_t}{N_b}\right){\theta_0}'' - S_c G_r{\varphi_0} = 0$$

The boundary conditions are:

$${f_1}''(0) = 0, {f_1}(0) = 0, {\theta_1}'(0) = 0, {\varphi_1}'(0) = 0 \; at \; \eta = 0 \quad (26)$$

$${f_1}'(1) = 0, {f_1}(1) = 0, {\theta_1}(1) = 0, {\varphi_1}(1) = 0 \; at \; \eta = 1 \quad (27)$$

Solving the above equations with their corresponding boundary conditions using maplesoftware.We would obtain:

$${f_0}(\eta) = -\tfrac{1}{2}\eta^3 + \tfrac{3}{2}\eta, {\theta_0}(\eta) = 1, {\varphi_0}(\eta) = 1 \quad (28)$$

The terms${f_i}(\eta)$, ${\theta_i}(\eta)$ and ${\varphi_i}(\eta)$ when $i \geq 1$ is too large that is mentioned graphically. The solution of equations is obtained when $p \to l$, will be as follows:

$$f(\eta) = {f_0}(\eta) + p^1{f_1}(\eta) + p^2{f_2}(\eta) \ldots = \sum_{i=0}^{N} p^i{f_i}(\eta) \quad (29)$$

$$\theta(\eta) = {\theta_0}(\eta) + p^1{\theta_1}(\eta) + p^2{\theta_2}(\eta) \ldots = \sum_{i=0}^{N} p^i{\theta_i}(\eta) \quad (30)$$

$$\varphi(\eta) = {\varphi_0}(\eta) + p^1{\varphi_1}(\eta) + p^2{\varphi_2}(\eta) \ldots = \sum_{i=0}^{N} p^i{\varphi_i}(\eta) \quad (31)$$

4 Analysis and Discussion of Results

4.1 Validation of code

In this work, HPM and RK-4 are applied to solve the problem. The present codes are validated by comparing the obtained results with the previously published results in the literaturewith $E_c = P_r = S_c = G_r = 1, H_a = 0 \text{and} \delta = 0.1$.As it is seen in **Tab 1**.This comparison illustratesthat the codes offer highly accurate solution for solving this problem. The results are very in good agreement.

Tab. 1 Comparison of values of $-f''(1)$ and $-\theta'(1)$ for different values of S

S	HAM [4]		DRA [5]		HPM (Present method)		NM	
	$-f''(1)$	$-\theta'(1)$	$-f''(1)$	$-\theta'(1)$	$-f''(1)$	$-\theta'(1)$	$-f''(1)$	$-\theta'(1)$
-1.0	2.170090	3.319899	2.170091	3.319888	2.170092	3.319860	2.170090	3.319899
-0.5	2.614038	3.129491	2.617403	3.129491	2.617403	3.129491	2.617403	3.129491
0.01	3.007134	3.047092	3.007133	3.047091	3.007133	3.047091	3.007133	3.047091
0.5	3.336449	3.026324	3.336449	3.026323	3.336449	3.026323	3.336449	3.026323
2.0	4.167389	3.118551	4.167041	3.113386	4.168065	3.127819	4.167389	3.118550

4.2 Discussion of Results

For more clarity and understanding of the problem, the results are interpreted in graphs for diverse values of pertaining parameters. The effect of squeezing number (S)on velocity, temperature, and concentration profiles is illustrated in the **Figs. 2 -5**, it's essential to notice that all figures are portrayed for the squeezing flow case $(S < 0)$ and the expanding flow case $(S > 0)$. It is discernible from **Figs.2-5** that both positive and negative squeeze numbers have different effects: From**Fig.2** the normal velocity profile decreases for $S > 0$, while it increases for $S < 0$, this is due to the fact that, when plates move apart from one another, the fluid is sucked into the channel which increases the velocity field. In another case, when plates move close to one another, fluid inside the channel is emitted out which gives the fluid dropping inside the channel and hence velocity of the fluid decreases. Also, from **Fig.3** the axial flow velocity profile decreased in the portion $0 \leq \eta \leq 0.45$, and it increases in the remaining part for the increasing values of $S > 0$. On the contrary it increases in the portion $0 \leq \eta \leq 0.45$ and it decreases in the remaining part for the increasing values of $S < 0$. Further in **Figs.4-5**, the temperature field decays and concentration profile increases for $S > 0$. While for $S > 0$ the temperature field increases and concentration profile decays.The decrease in the temperature field is due to the increased distance between the plates which can be relevant to the reduction in the kinematic viscosity or an increment in the speed which the plates move and therefore decrease the temperature field.

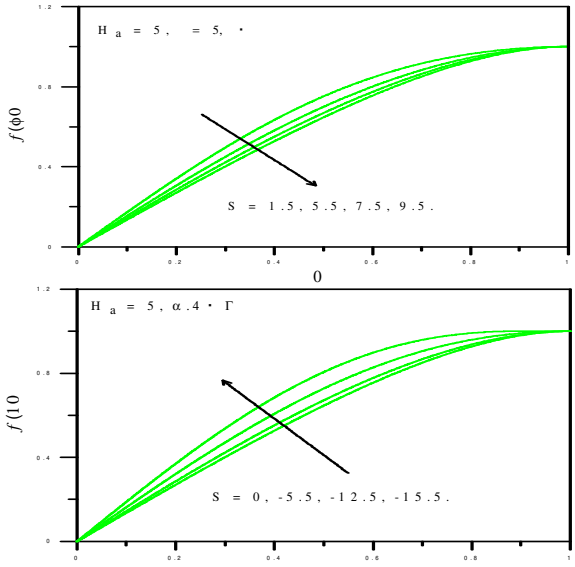

Fig. 2: impact of S on $f(\eta)$.

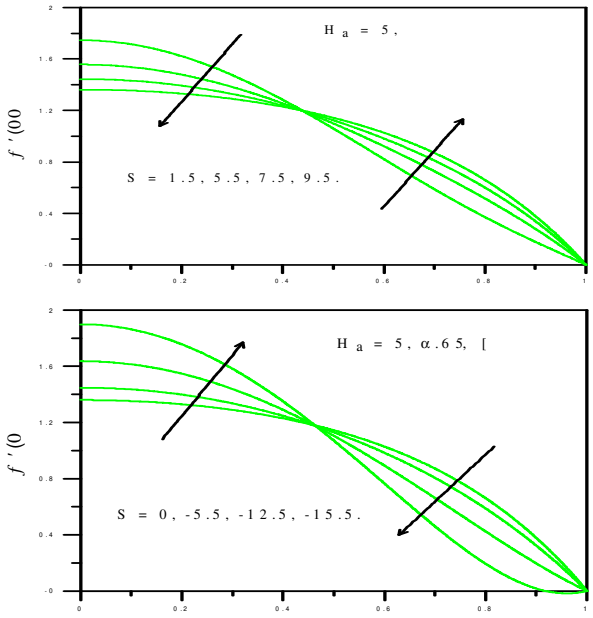

Fig. 3: impact of Son $f'(\eta)$

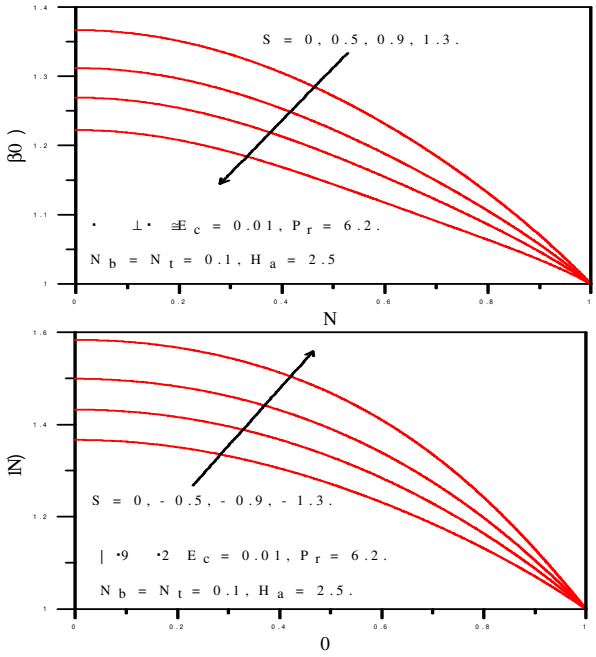

Fig. 4: impact of Son $\theta(\eta)$.

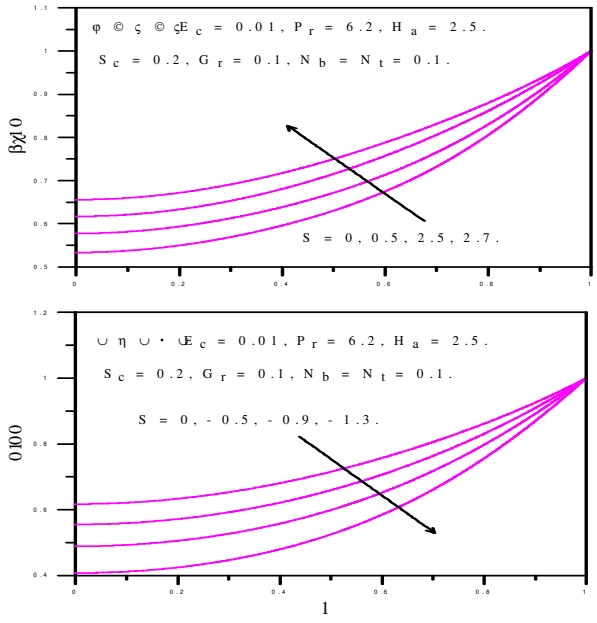

Fig. 5: impact of S on $\varphi(\eta)$.

The effect of Hartman number on velocity, temperature, and concentration profiles is depicted in the **Figs.6-9**.As it shown in the figures, as Hartman number H_a increases: the normal velocity profile in **Fig.6** decreases due to the presence of Lorentz forces which act against the flow, resistance to flow occurs and therefore the velocity field decreases. It is also noticed from **Fig.7** that, the axial velocity field decreases in the region $0 \leq \eta \leq 0.45$, while it increases in the remaining part. On the other hand, **Fig.8** displays that, temperature field grows. Further, from **Fig.9** it is observed that, the concentration rises.

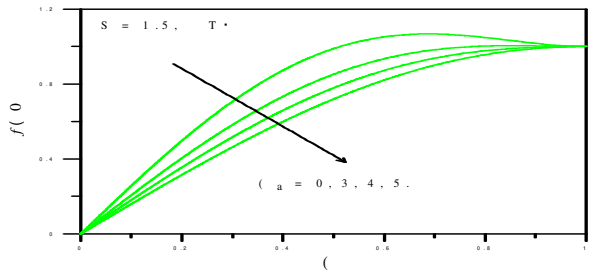

Fig. 6: impact of H_a on $f(\eta)$.

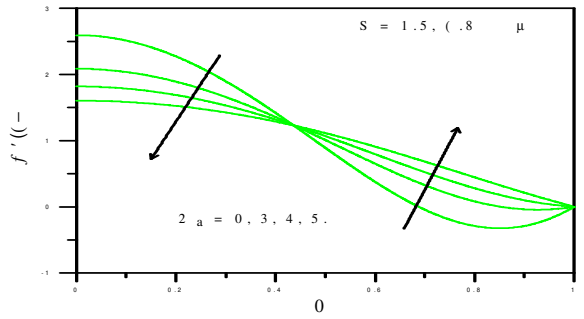

Fig. 7: impact of H_a on $f'(\eta)$.

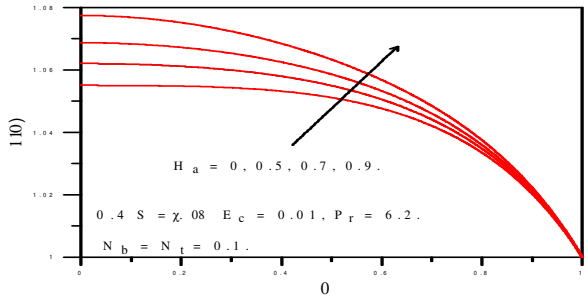

Fig. 8: *impact of* H_a*on* $\theta(\eta)$.

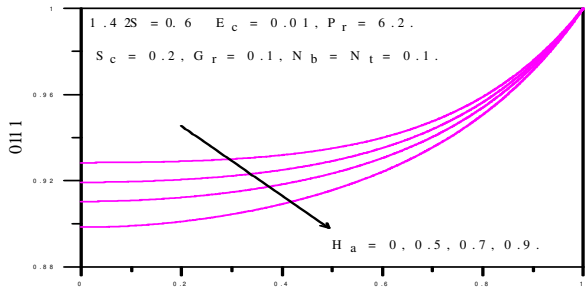

Fig. 9: *impact of* H_a*on* $\varphi(\eta)$.

The impact of Casson fluid parameter βon velocity, temperature, and concentration profiles is depicted in the **Figs.10-13**. When the Casson fluid parameter β rises: according to **Fig.10**the normal velocity decreases, because under the influence of applied stresses, the small increase of βincreases the viscosity of the nanofluid and thus the normal velocitydecreases. Moreover, it is noticed from **Fig.11** that the axial velocity profile is decreased in the portion$0 \leq \eta \leq 0.45$, on the contrary it increases in the remaining part. Further, from **Fig.12**temperature field decreases, and in the **Fig.13** is observed that, the concentration rises.

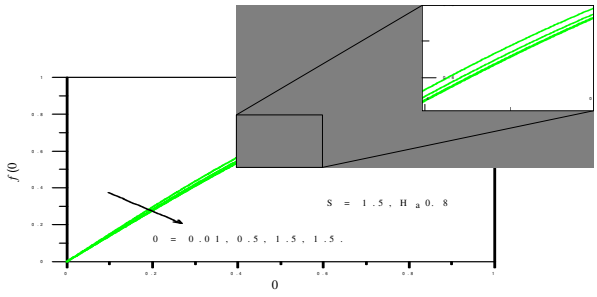

Fig. 10: impact of β on $f(\eta)$.

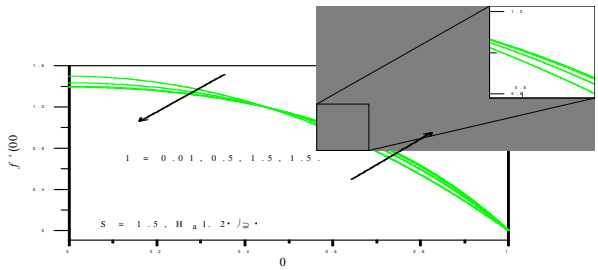

Fig. 11: impact of β on $f'(\eta)$.

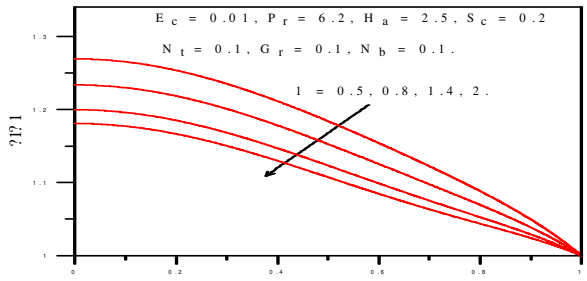

Fig.12:*impact of* β *on* $\theta(\eta)$.

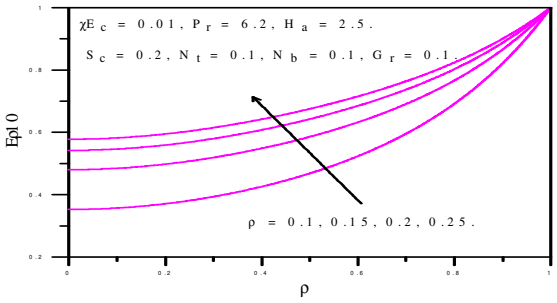

Fig.13:*impact of* β *on* $\varphi(\eta)$.

Influence of Thermophoresis parameter N_t and Brownian motion parameter N_b on concentration profile is portrayed in the **Figs.13-14**.From the **Fig.13**, it can be seen that the concentration profile decreases with increase theN_t. This situation is due to the appearance of stronger thermophoresis forces in the flow region. On the contrary in **Fig.14**, it increases with increase the N_b.

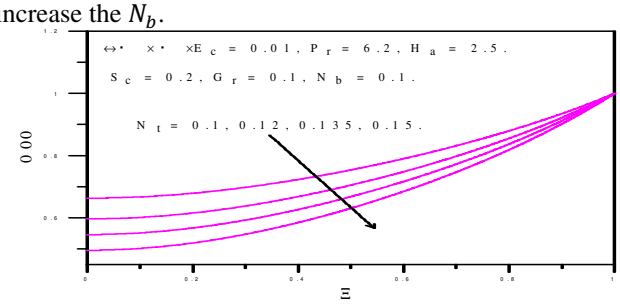

Fig. 14*:impact of* $N_t on \varphi(\eta)$.

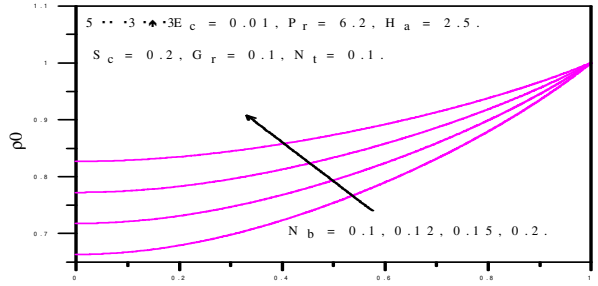

Fig. 15:impact of $N_b$on $\varphi(\eta)$.

The effect of time-dependent chemical reaction parameter $G_r$and Schmidt number S_c on concentration profile is depicted in the **Figs.16-17**. It is observed from **Fig.16**that both positive and negative time-dependent chemical reaction parameter have different effects on the concentration profile. For$G_r > 0$the concentration profile reduces because of the destruction of chemical reaction.While it increases for $G_r<0$ because of the generation of chemical reaction. On the otherwise from **Fig.17** the concentration distribution reduces with rising S_c.

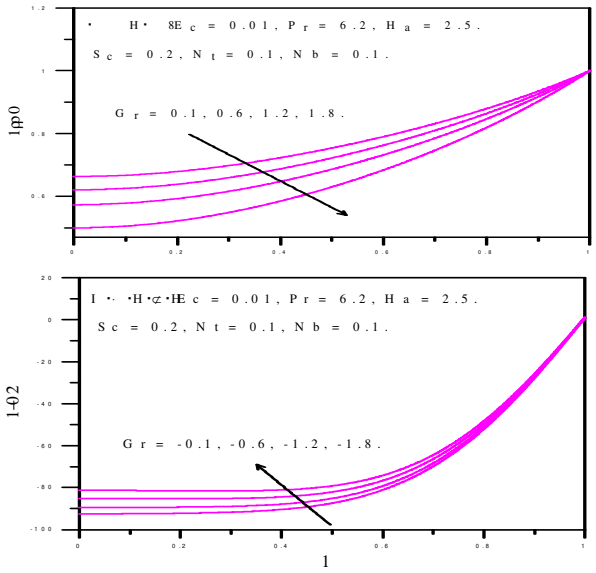

Fig. 16:*impact of* $G_r on \varphi(\eta)$.

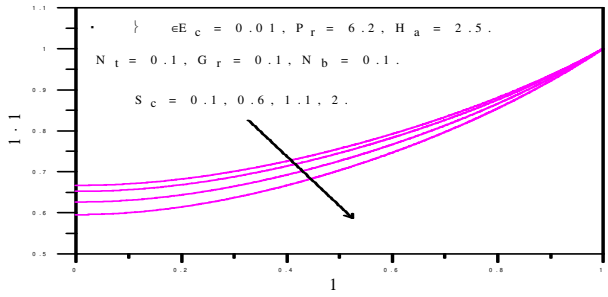

Fig. 17:*impactof*$S_c on \varphi(\eta)$.

5 Conclusion

This work is presented to study the arterial blood flow with nanoparticles in a magnetic field due to the squeezing action of the heart.The study was treated as a casson nanofluid flowing between two parallel plates placed at a distance varying in time under the influence of a uniform magnetic field with variable chemical reaction. HPM and RK4 have been used to solve the governing equations.The effects of important parameters involved have been discussed and presented in graphs.As a major conclusion of this study,it is established thatthe magnetic field has the ability to reduce the velocityof blood flow in the arteries so it can be used as a flow control.Also, positive and negative squeeze numbers have opposite effects on heat and mass transfer flow throughout all the cases.Whereasthe concentration of nanoparticles increases with Brownian motion while thermophoresis phenomenon has the opposite effect.

References

1. Xuan, Y., & Li, Q. (2000). Heat transfer enhancement of nanofluids. *International Journal of heat and fluid flow*, *21*(1), 58-64
2. Choi, S. U., & Eastman, J. A. (1995). *Enhancing thermal conductivity of fluids with nanoparticles* (No. ANL/MSD/CP-84938; CONF-951135-29). Argonne National Lab., IL (United States).
3. Buongiorno, J. (2006). Convective transport in nanofluids.
4. Prakash, M., &Giannelis, E. P. (2007). Mechanism of heat transport in nanofluids. *Journal of computer-aided materials design*, *14*(1), 109-117.
5. Sheikholeslami, M., &Ganji, D. D. (2014). Numerical investigation for two phase modeling of nanofluid in a rotating system with permeable sheet. *Journal of Molecular Liquids*, *194*, 13-19.
6. Stefan, J. (1875). Versucheüber die scheinbareAdhäsion. *Annalen der Physik*, *230*(2), 316-318.
7. Domairry, G., & Aziz, A. (2009). Approximate analysis of MHD squeeze flow between two parallel disks with suction or injection by homotopy perturbation method. *Mathematical Problems in Engineering*, *2009*.
8. Mahmood, M., Asghar, S., & Hossain, M. A. (2007). Squeezed flow and heat transfer over a porous surface for viscous fluid. *Heat and mass Transfer*, *44*(2), 165-173.
9. Mustafa, M., Hayat, T., &Obaidat, S. (2012). On heat and mass transfer in the unsteady squeezing flow between parallel plates. *Meccanica*, *47*(7), 1581-1589.
10. Dogonchi, A. S., &Ganji, D. D. (2016). Investigation of MHD nanofluid flow and heat transfer in a stretching/shrinking convergent/divergent channel considering thermal radiation. *Journal of Molecular Liquids*, *220*, 592-603.
11. Sheikholeslami, M., Abelman, S., &Ganji, D. D. (2014). Numerical simulation of MHD nanofluid flow and heat transfer considering viscous dissipation. *International Journal of Heat and Mass Transfer*, *79*, 212-222.
12. McDonald, D. A. Blood flow in arteries. 1974. *Edward Arnold, London*, 92-95.
13. Eldabe, N. T. M., Saddeck, G., & El-Sayed, A. F. (2001). Heat transfer of MHD non-Newtonian Casson fluid flow between two rotating cylinders. *Mechanics and Mechanical Engineering*, *5*(2), 237-251.
14. Boyd, J., Buick, J. M., & Green, S. (2007). Analysis of the Casson and Carreau-Yasuda non-Newtonian blood models in steady and oscillatory flows using the lattice Boltzmann method. *Physics of Fluids*, *19*(9), 093103.
15. Fredrickson, A. G. (1964). *Principles and applications of rheology*. Prentice-Hall.
16. Mustefa, M., Hayet, T., Pop, I., & Aziz, A. (2011). Unstedybounderylayar flow of a Casson fluid impulsively startad moving fletplte. *Heat Transfer–Asian Ras*, *40*(6), 563-76.
17. Sheikholeslami, M., Azimi, M., &Ganji, D. D. (2015). Application of differential transformation method for nanofluid flow in a semi-permeable channel considering magnetic field effect. *International Journal for Computational Methods in Engineering Science and Mechanics*, *16*(4), 246-255.
18. Jang, M. J., Chen, C. L., & Liu, Y. C. (2001). Two-dimensional differential transform for partial differential equations. *Applied Mathematics and Computation*, *121*(2-3), 261-270.
19. Mohyud-Din, S. T., & Yildirim, A. (2010). Ma's variation of parameters method for Fisher's equations. *Advances in Applied Mathematics and Mechanics*, *2*(3), 379-388.
20. Sheikholeslami, M., Ellahi, R., Ashorynejad, H. R., Domairry, G., & Hayat, T. (2014). Effects of heat transfer in flow of nanofluids over a permeable stretching wall in a porous medium. *Journal of Computational and Theoretical Nanoscience*, *11*(2), 486-496.
21. Sheikholeslami, M., Ganji, D. D., &Ashorynejad, H. R. (2013). Investigation of squeezing unsteady nanofluid flow using ADM. *Powder Technology*, *239*, 259-265.
22. Sheikholeslami, M., &Ganji, D. D. (2013). Heat transfer of Cu-water nanofluid flow between parallel plates. *Powder Technology*, *235*, 873-879.
23. He, J. H. (2000). A new perturbation technique which is also valid for large parameters. *Journal of Sound and Vibration*, *229*(5), 1257-1263.
24. Rohlf, K., &Tenti, G. (2001). The role of the Womersley number in pulsatile blood flow: a theoretical study of the Casson model. *Journal of biomechanics*, *34*(1), 141-148.
25. Lohmann, T., Bock, H. G., &Schloeder, J. P. (1992). Numerical methods for parameter estimation and optimal experiment design in chemical reaction systems. *Industrial & engineering chemistry research*, *31*(1), 54-57.
26. Rapp, B. E. (2016). *Microfluidics: modeling, mechanics and mathematics*. William Andrew.
27. Sheikholeslami, M., &Ganji, D. D. (2016). *External magnetic field effects on hydrothermal treatment of nanofluid: numerical and analytical studies*. William Andrew.
28. El Harfouf, A., Wakif, A., & Mounir, S. H. (2020). Heat Transfer Analysis on Squeezing Unsteady MHD Nanofluid Flow Between Two Parallel Plates Considering Thermal Radiation, Magnetic and Viscous Dissipations Effects a Solution by Using Homotopy Perturbation Method. *Sensor Letters*, *18*(2), 113-121.